# A Diffusion Remote Microphone Technique for Distributed Active Noise Control

Tianyou Li[*], Sipei Zhao[†], Haowen Li[*], Xiaofeng Zeng[*], Ruquan Sun[*] and Jing Lu[*]
[*] Key Laboratory of Modern Acoustics and Institute of Acoustics, Nanjing University, Nanjing, China
E-mail: {tianyou.li, haowenli, xiaofeng.zeng, ruquan.sun} @smail.nju.edu.cn, lujing@nju.edu.cn
[†] CAAV, Faculty of Engineering and IT, University of Technology Sydney, Sydney, Australia
E-mail: sipei.zhao@uts.edu.au

***Abstract*— The well-known Remote Microphone Technique (RMT) creates quiet zones at locations away from physical microphones, making it suitable for active noise control (ANC) in large-scale open environments. Conventional centralized RMT algorithms rely on a single processor for multi-point noise prediction and global control filter updates. However, the resulting high computational cost limits scalability in practical applications. Recently, distributed RMT approaches based on incremental strategies have been proposed, where each node in the acoustic device network performs local noise prediction and participates in global filter estimation, thereby distributing the computational load across the system. However, the serial communication mechanism inherent to incremental strategies increases vulnerability to link failures and leads to excessive communication latency, which may violate ANC causality constraints and degrade noise reduction performance. This paper proposes a distributed RMT scheme based on an augmented diffusion strategy. By leveraging neighborhood cooperation and parallel communication, the proposed method reduces computational complexity and significantly shortens communication latency. Simulation results and system complexity analyses demonstrate that it achieves consistent steady-state noise reduction performance with significantly lower computational and communication costs.**

## I. INTRODUCTION

Active noise control (ANC) has been extensively studied as an effective approach for mitigating low-frequency noise in various acoustic environments, including vehicle cabins [1, 2], aircraft [3], and open spaces [4]. Among ANC techniques, the Remote Microphone Technique (RMT) has attracted significant attention due to its ability to attenuate noise at target positions without deploying physical microphones [5]. RMT estimates the virtual error signals at virtual microphones, which represents residual noise signals at the target listening points, by using the physical error signals measured by physical microphones and the loudspeaker output signals. The estimated signals are then used to update the control filters, which adjust the loudspeaker output signals to achieve noise reduction [6].

Conventional centralized RMT (CRMT) schemes iteratively update global control filters based on the estimated virtual error signals [7]. Although CRMT exhibits robust convergence and noise reduction performance, its high computational complexity limits scalability and flexibility in practical systems with a massive number of loudspeakers and microphones.

To reduce the system computational burden, a distributed RMT algorithm based on incremental strategies has been proposed [8]. Incremental RMT (IRMT) distributes the computational tasks of a centralized processor across distributed nodes through serial communication and collaborative processing mechanisms [9]. Each node locally estimates the global control filter using its own microphone and loudspeaker signals. Although IRMT effectively reduces the computational load on a single processor, its serial communication topology increases vulnerability to link failures and may introduce excessive latency, which degrades noise reduction performance.

In contrast, diffusion strategies employ a parallel communication mechanism, where each node can establish direct communication links with others in real-time distributed ANC systems [10]. Single-task [11] and multi-task [12] diffusion strategies were among the earliest control approaches. However, the former aims to optimize global control filter, leading to higher computational complexity at each node, while the latter focuses on local control filter but enforces similarity across nodes, which may degrade noise reduction performance under asymmetrical acoustic paths. To overcome these limitations, an augmented diffusion strategy was developed [13, 14], in which each node optimizes an augmented control filter consisting of its own and neighboring nodes' control filters. Through neighborhood-wide adaptation and node-specific combination, this strategy maintains effective noise reduction with low computational complexity. However, its steady-state performance remains sensitive to the combination rule. To improve robustness, a constant edge-weighted combination rule was introduced for real-time distributed ANC systems [15]. Furthermore, a mixed-gradient diffusion strategy with compensation filtering has demonstrated improved robustness and resilience to communication delays [16].

Most existing diffusion-based ANC algorithms are designed to minimize error signals at physical microphone positions and

979-8-3315-7206-8/25/$31.00 ©2025 IEEE

do not fully address the unique challenges of RMT. This paper proposes an augmented diffusion-based RMT (ADRMT) scheme that achieves virtual error signal estimation and noise reduction at target listening positions through network-wide adaptation, neighborhood-wide adaptation, and node-specific combination. Simulations on an 8-channel ANC headrest system show that the proposed ADRMT achieves noise reduction performance comparable to existing centralized and incremental RMT schemes, while requiring lower computational complexity and communication latency.

Notation: Italic letters (e.g., $x$, $X$) denote scalars. Boldface lower-case (e.g., $\mathbf{x}$) and capital letters (e.g., $\mathbf{X}$) denote vectors and matrices, respectively. The superscript $(\bullet)^{\mathrm{T}}$ denotes transpose, and $\|\bullet\|^2$ represents the $\ell_2$-norm. The operator $\mathrm{col}\{\bullet\}$ stacks its vector arguments as a column vector. The operator $\mathbb{E}[\bullet]$ denotes the statistical expectation.

## II. Existing Remote Microphone Techniques

### A. System Model

Consider the ANC headrest system illustrated in Fig. 1, where $A$ pairs of secondary loudspeakers and physical microphones are deployed to suppress the primary noise at $A$ target listening positions (i.e., virtual microphones) without microphones. This paired loudspeaker-microphone configuration is used to clearly illustrate the algorithmic process of the proposed Augmented Diffusion Remote Microphone Technique, which can also be extended to non-paired configurations via the extended augmented diffusion strategy [15]. Before ANC operation, measurement microphones are temporarily placed at the target listening positions to identify the observation acoustic paths between the physical microphones and target listening positions using the least-squares method [17]. During ANC operation, these microphones are removed, and the pre-measured paths are used to predict residual noise at the target listening positions, enabling virtual microphone-based noise suppression.

The virtual error signal at the $a$-th virtual microphone at time instant $n$ is estimated by

$$\hat{e}_{\mathbf{v},a}(n) = \hat{b}_{\mathbf{v},a}(n) + \sum_{l=1}^{A} \hat{\mathbf{q}}_{(\mathbf{v},a),l}^{\mathrm{T}} \mathbf{g}_l(n), \tag{1}$$

where $\hat{b}_{\mathbf{v},a}(n)$ represents the estimated primary noise at the $a$-th virtual microphone. $\hat{\mathbf{q}}_{(\mathbf{v},a),l} \in \mathbb{R}^{Q\times 1}$ denotes the measured acoustic path between the $a$-th virtual microphone and the $l$-th secondary loudspeaker, modeled as an FIR filter with $Q$ taps, which can be identified through either offline or online path measurement techniques [18]. $\mathbf{g}_l(n) \in \mathbb{R}^{Q\times 1}$ is the output signal vector of the $l$-th secondary loudspeaker.

The primary noise $\hat{b}_{\mathbf{v},a}(n)$ is estimated from the physical microphone signals and the observation acoustic paths by

$$\hat{b}_{\mathbf{v},a}(n) = \sum_{c=1}^{A} \hat{\mathbf{r}}_{(\mathbf{v},a),(\mathbf{p},c)}^{\mathrm{T}} \hat{\mathbf{b}}_{\mathbf{p},c}(n), \tag{2}$$

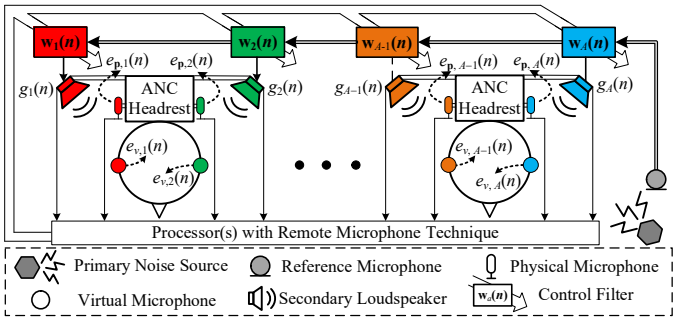

Fig. 1 Block diagram of the ANC headrest system.

where $\hat{\mathbf{r}}_{(\mathbf{v},a),(\mathbf{p},c)}^{\mathrm{T}} \in \mathbb{R}^{R\times 1}$ represents the pre-measured observation acoustic path with $R$ taps between the $c$-th physical microphone and the $a$-th virtual microphone. $\hat{\mathbf{b}}_{\mathbf{p},c}(n) \in \mathbb{R}^{R\times 1}$ denotes the estimated primary noise signal at the $c$-th physical microphone, which is computed as

$$\hat{b}_{\mathbf{p},c}(n) = e_{\mathbf{p},c}(n) - \sum_{l=1}^{A} \hat{\mathbf{q}}_{(\mathbf{p},c),l}^{\mathrm{T}} \mathbf{g}_l(n), \tag{3}$$

where $e_{\mathbf{p},c}(n)$ is the physical error signal measured at the $c$-th physical microphone. $\hat{\mathbf{q}}_{(\mathbf{p},c),l}$ denotes the measured acoustic path between the $c$-th physical microphone and the $l$-th secondary loudspeaker. By substituting (2) and (3) into (1), the estimated virtual error signal is expressed as

$$\hat{e}_{\mathbf{v},a}(n) = \sum_{c=1}^{A} \hat{\mathbf{r}}_{(\mathbf{v},a),(\mathbf{p},c)}^{\mathrm{T}} \mathbf{e}_{\mathbf{p},c}(n) - \sum_{l=1}^{A} \hat{\mathbf{s}}_{(\mathbf{v},a),l}^{\mathrm{T}} \mathbf{g}_l(n), \tag{4}$$

where $\mathbf{e}_{\mathbf{p},c}(n) \in \mathbb{R}^{R\times 1}$ denotes the physical error signal vector. $\hat{\mathbf{s}}_{(\mathbf{v},a),l} \in \mathbb{R}^{(R+Q-1)\times 1}$ represents the cascaded acoustic path, obtained by convolving $\hat{\mathbf{r}}_{(\mathbf{v},a),(\mathbf{p},c)}^{\mathrm{T}}$, $\hat{\mathbf{q}}_{(\mathbf{p},c),l}$ and $\hat{\mathbf{q}}_{(\mathbf{v},a),l}$. Equation (4) indicates that the physical error signals and loudspeaker output signals can be jointly used to estimate the virtual error signals, which are then employed to update the loudspeaker output signals for noise suppression at the target positions.

### B. Centralized Remote Microphone Technique

As illustrated in Fig. 2(a), the conventional Centralized RMT (CRMT) first collects the global physical error signal and global loudspeaker output signal to estimate the global virtual error signal. The global control filter is then updated based on the estimated global virtual error signal, and the loudspeaker outputs are subsequently adjusted to achieve noise reduction.

Quantitatively, the essence of the CRMT lies in minimizing the true noise at the target listening positions under the assumption that the estimated global virtual error signals $\hat{\mathbf{E}}_{\mathbf{v}}(n)$ are sufficiently accurate. Thus, CRMT uses a cost function consistent with classical centralized strategies for broadband [19] and narrowband [20] noise reduction.

$$J^{\mathrm{C}}(\mathbf{w}) = \mathbb{E}\left[\mathbf{E}_{\mathbf{v}}^{\mathrm{T}}(n)\mathbf{E}_{\mathbf{v}}(n)\right], \tag{5}$$

where $\mathbf{E}_{\mathbf{v}}(n)$ is the true global virtual error signal vector. According to (1) and Ref. [21], the true global virtual error signal can be expressed in filtered-reference matrix form as

$$\underbrace{\begin{bmatrix} e_{\mathrm{v},1}(n) \\ e_{\mathrm{v},2}(n) \\ \vdots \\ e_{\mathrm{v},A}(n) \end{bmatrix}}_{\mathbf{E}_{\mathrm{v}}(n)} = \underbrace{\begin{bmatrix} \mathbf{x}_{\mathbf{F},(1,1)}^{\mathrm{T}}(n) & \mathbf{x}_{\mathbf{F},(1,2)}^{\mathrm{T}}(n) & \cdots & \mathbf{x}_{\mathbf{F},(1,A)}^{\mathrm{T}}(n) \\ \mathbf{x}_{\mathbf{F},(2,1)}^{\mathrm{T}}(n) & \mathbf{x}_{\mathbf{F},(2,2)}^{\mathrm{T}}(n) & \cdots & \mathbf{x}_{\mathbf{F},(2,A)}^{\mathrm{T}}(n) \\ \vdots & \vdots & \ddots & \vdots \\ \mathbf{x}_{\mathbf{F},(A,1)}^{\mathrm{T}}(n) & \mathbf{x}_{\mathbf{F},(A,2)}^{\mathrm{T}}(n) & \cdots & \mathbf{x}_{\mathbf{F},(A,A)}^{\mathrm{T}}(n) \end{bmatrix}}_{\mathbf{X}_{\mathbf{v},\mathbf{l}}} \times \underbrace{\begin{bmatrix} \mathbf{w}_1(n) \\ \mathbf{w}_2(n) \\ \vdots \\ \mathbf{w}_A(n) \end{bmatrix}}_{\mathbf{w}(n)} + \underbrace{\begin{bmatrix} b_{\mathrm{v},1}(n) \\ b_{\mathrm{v},2}(n) \\ \vdots \\ b_{\mathrm{v},A}(n) \end{bmatrix}}_{\mathbf{B}_{\mathrm{v}}(n)}. \tag{6}$$

where $\mathbf{w}_l \in \mathbb{R}^{U\times 1}$ denotes the control filter for the $l$-th loudspeaker, which filters the reference signal $\mathbf{x}(n)=[x(n) \quad x(n-1) \quad \cdots \quad x(n-U+1)]^{\mathrm{T}}$ to generate the corresponding loudspeaker output signal $g_l(n)=\mathbf{w}_l^{\mathrm{T}}(n)\mathbf{x}(n)$. The vector $\mathbf{B}_{\mathrm{v}}(n)$ denotes the true primary noise at the virtual microphone positions. The filtered-reference matrix $\mathbf{X}_{\mathbf{v},\mathbf{l}}$ contains the filtered-reference signals obtained by filtering the reference signal through the acoustic path between the virtual microphone and the loudspeaker. Its sub-vector is defined as $\mathbf{x}_{\mathbf{F},(v,l)}=[x_{\mathbf{F},(v,l)}(n) \quad x_{\mathbf{F},(v,l)}(n-1) \quad \cdots \quad x_{\mathbf{F},(v,l)}(n-U+1)]^{\mathrm{T}}$, where $x_{\mathbf{F},(v,l)}(n)=[x(n) \quad x(n-1) \quad \cdots \quad x(n-Q+1)]\mathbf{q}_{(\mathbf{v},v),l}$, and $\mathbf{q}_{(\mathbf{v},v),l}$ denotes the acoustic path between the $v$-th virtual microphone and the $l$-th secondary loudspeaker. The global control filters are updated using the stochastic gradient descent algorithm as

$$\mathbf{w}(n+1)=\mathbf{w}(n)-\mu^{\mathrm{C}}\hat{\mathbf{X}}_{\mathbf{v},\mathbf{l}}^{\mathrm{T}}(n)\mathbf{E}_{\mathrm{v}}(n), \tag{7}$$

where $\mu^{\mathrm{C}}$ is the step-size of the CRMT, and $\hat{\mathbf{X}}_{\mathbf{v},\mathbf{l}}(n)$ is the estimated filtered-reference signal matrix with the measured acoustic path.

According to (4), the global virtual error signal $\mathbf{E}_{\mathrm{v}}(n)$ in (7) can be estimated by using the global physical error signals $\mathbf{E}_{\mathbf{p}}(n)$ and the global loudspeaker output signals $\mathbf{G}(n)$ as

$$\underbrace{\begin{bmatrix} \hat{e}_{\mathbf{v},1}(n) \\ \hat{e}_{\mathbf{v},2}(n) \\ \vdots \\ \hat{e}_{\mathbf{v},A}(n) \end{bmatrix}}_{\hat{\mathbf{E}}_{\mathbf{v}}(n)} = \underbrace{\begin{bmatrix} \hat{\mathbf{r}}_{(\mathbf{v},1),(\mathbf{p},1)}^{\mathrm{T}} & \hat{\mathbf{r}}_{(\mathbf{v},1),(\mathbf{p},2)}^{\mathrm{T}} & \cdots & \hat{\mathbf{r}}_{(\mathbf{v},1),(\mathbf{p},A)}^{\mathrm{T}} \\ \hat{\mathbf{r}}_{(\mathbf{v},2),(\mathbf{p},1)}^{\mathrm{T}} & \hat{\mathbf{r}}_{(\mathbf{v},2),(\mathbf{p},2)}^{\mathrm{T}} & \cdots & \hat{\mathbf{r}}_{(\mathbf{v},2),(\mathbf{p},A)}^{\mathrm{T}} \\ \vdots & \vdots & \ddots & \vdots \\ \hat{\mathbf{r}}_{(\mathbf{v},A),(\mathbf{p},1)}^{\mathrm{T}} & \hat{\mathbf{r}}_{(\mathbf{v},A),(\mathbf{p},2)}^{\mathrm{T}} & \cdots & \hat{\mathbf{r}}_{(\mathbf{v},A),(\mathbf{p},A)}^{\mathrm{T}} \end{bmatrix}}_{\hat{\mathbf{R}}_{\mathbf{v},\mathbf{p}}} \underbrace{\begin{bmatrix} \mathbf{e}_{\mathbf{p},1}(n) \\ \mathbf{e}_{\mathbf{p},2}(n) \\ \vdots \\ \mathbf{e}_{\mathbf{p},A}(n) \end{bmatrix}}_{\mathbf{E}_{\mathbf{p}}(n)} - \underbrace{\begin{bmatrix} \hat{\mathbf{s}}_{(\mathbf{v},1),1}^{\mathrm{T}} & \hat{\mathbf{s}}_{(\mathbf{v},1),2}^{\mathrm{T}} & \cdots & \hat{\mathbf{s}}_{(\mathbf{v},1),A}^{\mathrm{T}} \\ \hat{\mathbf{s}}_{(\mathbf{v},2),1}^{\mathrm{T}} & \hat{\mathbf{s}}_{(\mathbf{v},2),2}^{\mathrm{T}} & \cdots & \hat{\mathbf{s}}_{(\mathbf{v},2),A}^{\mathrm{T}} \\ \vdots & \vdots & \ddots & \vdots \\ \hat{\mathbf{s}}_{(\mathbf{v},A),1}^{\mathrm{T}} & \hat{\mathbf{s}}_{(\mathbf{v},A),2}^{\mathrm{T}} & \cdots & \hat{\mathbf{s}}_{(\mathbf{v},A),A}^{\mathrm{T}} \end{bmatrix}}_{\mathbf{S}_{\mathbf{v},\mathbf{G}}} \underbrace{\begin{bmatrix} \mathbf{g}_1(n) \\ \mathbf{g}_2(n) \\ \vdots \\ \mathbf{g}_A(n) \end{bmatrix}}_{\mathbf{G}(n)}. \tag{8}$$

The estimated virtual error signal in (8) is then used to update the global control filter as defined in (7), which yields the conventional CRMT update formula given by

$$\mathbf{w}(n+1)=\mathbf{w}(n)-\mu^{\mathrm{C}}\hat{\mathbf{X}}_{\mathbf{v},\mathbf{l}}^{\mathrm{T}}(n)\hat{\mathbf{E}}_{\mathrm{v}}(n). \tag{9}$$

Equations (8) and (9) show that CRMT estimates the global virtual error signal and updates global control filter in each iteration, resulting in high computational complexity.

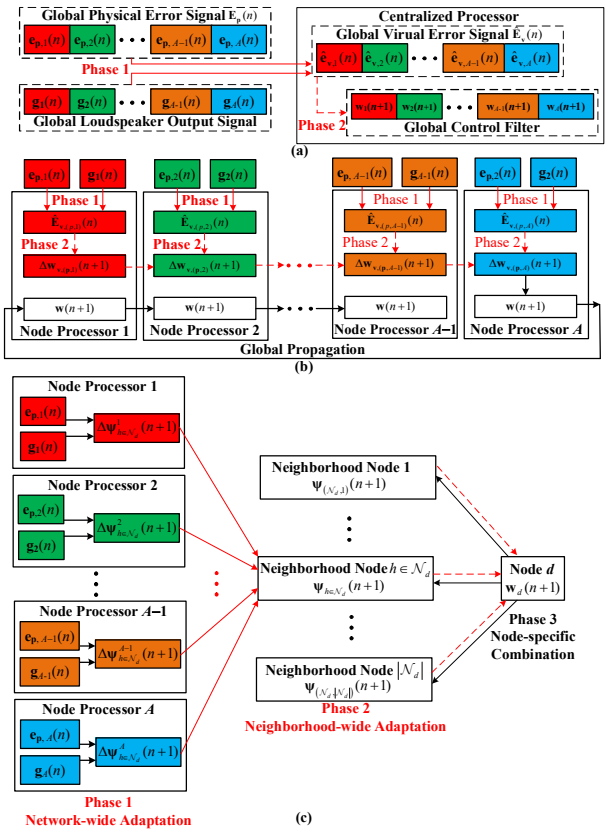


Fig. 2 Block diagrams of (a) CRMT, (b) IRMT, and (c) ADRMT strategies implemented in ANC headrest systems.

### C. *Incremental Remote Microphone Technique*

As shown in Fig. 2(b), the Incremental Remote Microphone Technique (IRMT) structures the system as a distributed node network with serial communication. In each iteration, each node estimates the global virtual error signal from local acoustic signals, updates the global control filter, and passes the result to the next node. After all local updates, a global propagation phase sequentially delivers the final control filter to all nodes for the next iteration.

Specifically, the global virtual error signal in (8) can be written as an incremental sum of local estimates, given by

$$\hat{\mathbf{E}}_{\mathrm{v}}(n)=\sum_{d=1}^{A}\hat{\mathbf{E}}_{\mathbf{v},(\mathbf{p},d)}(n)=\sum_{d=1}^{A}\left[\mathbf{R}_{\mathbf{v},(\mathbf{p},d)}\mathbf{e}_{\mathbf{p},d}(n)-\mathbf{S}_{\mathbf{v},(\mathbf{G},d)}\mathbf{g}_d(n)\right], \tag{10}$$

where $\hat{\mathbf{E}}_{\mathbf{v},(\mathbf{p},d)}(n)=[\hat{e}_{(\mathbf{v},1)(\mathbf{p},d)}(n) \quad \hat{e}_{(\mathbf{v},2)(\mathbf{p},d)}(n) \quad \cdots \quad \hat{e}_{(\mathbf{v},A)(\mathbf{p},d)}(n)]^{\mathrm{T}}$ and $\hat{e}_{(\mathbf{v},a)(\mathbf{p},d)}(n)$ represents the estimated virtual error signal at the $a$-th virtual microphone using the physical error signal and loudspeaker output signal of the $d$-th node. The matrices are defined as $\mathbf{R}_{\mathbf{v},(\mathbf{p},d)}=[\hat{\mathbf{r}}_{(\mathbf{v},1),(\mathbf{p},d)} \quad \hat{\mathbf{r}}_{(\mathbf{v},2),(\mathbf{p},d)} \quad \cdots \quad \hat{\mathbf{r}}_{(\mathbf{v},A),(\mathbf{p},d)}]^{\mathrm{T}}$ and $\mathbf{S}_{\mathbf{v},(\mathbf{G},d)}=[\hat{\mathbf{s}}_{(\mathbf{v},1),d} \quad \hat{\mathbf{s}}_{(\mathbf{v},2),d} \quad \cdots \quad \hat{\mathbf{s}}_{(\mathbf{v},A),d}]^{\mathrm{T}}$, which are the sub-vectors of $\mathbf{R}_{\mathbf{v},\mathbf{p}}$ and $\mathbf{S}_{\mathbf{v},\mathbf{G}}$ in (8), respectively.

By substituting (10) into (9), the global control filter update can be rewritten as

$$\begin{aligned}\mathbf{w}(n+1)&=\mathbf{w}(n)-\mu^{\mathrm{C}}\hat{\mathbf{X}}_{\mathbf{v},\mathbf{l}}^{\mathrm{T}}(n)\sum_{d=1}^{A}\hat{\mathbf{E}}_{\mathbf{v},(\mathbf{p},d)}(n)\\&=\mathbf{w}(n)-\sum_{d=1}^{A}\left[\mu^{\mathrm{C}}\hat{\mathbf{X}}_{\mathbf{v},\mathbf{l}}^{\mathrm{T}}(n)\hat{\mathbf{E}}_{\mathbf{v},(\mathbf{p},d)}(n)\right]\\&=\mathbf{w}(n)-\sum_{d=1}^{A}\Delta\mathbf{w}_{\mathbf{v},(\mathbf{p},d)}(n+1),\end{aligned} \tag{11}$$

where $\Delta\mathbf{w}_{\mathbf{v},(\mathbf{p},d)}(n+1)$ denotes the contribution of node $d$ to the global control filter update. As observed from (11), the IRMT scheme distributes the computational load across all nodes, thereby alleviating the burden on a centralized processor. Essentially, IRMT decomposes the global update expression of CRMT in (9) into an incremental accumulation of local updates computed at each node. Under ideal conditions without communication delays or constraints, IRMT can achieve convergence speed and noise reduction performance consistent with those of CRMT.

## III. Proposed Augmented Diffusion Remote Microphone Technique

The algorithm flow of the proposed Augmented Diffusion Remote Microphone Technique (ADRMT) is illustrated in Fig. 2(c). Unlike the serial communication architecture used in IRMT, ADRMT adopts parallel communication architecture to alleviate link failure issues and reduce communication latency.

Fig. 2(c) illustrates that the update of node $d$'s control filter involves three phases: network-wide adaptation, neighborhood-wide adaptation, and node-specific combination. In the network-wide adaptation phase, all nodes utilize their local physical error signals and loudspeaker output signals to estimate the augmented control filters for the neighborhood $\mathcal{N}_d$ of node $d$, and transmit the estimated results to the neighboring nodes $\mathcal{N}_d$. In the neighborhood-wide adaptation phase, the neighboring nodes $\mathcal{N}_d$ aggregate the received estimates and update the augmented control filters accordingly. In the node-specific combination phase, node $d$ receives the updated control filter estimates from its neighboring nodes $\mathcal{N}_d$, combines them with its own control filter estimates to update its own control filter, and then transmits the updated result back to the neighboring nodes $\mathcal{N}_d$ to initialize the next iteration of the neighborhood-wide adaptation phase.

Quantitatively, the cost function of the conventional Augmented Diffusion algorithm [22, 23] is defined as

$$\begin{aligned} J_d^{\mathrm{AD}}(\boldsymbol{\varphi}_d) &= \mathbb{E}\left[e_{\mathbf{v},d}^2(n)\right] + \lambda_d \sum_{h\in\mathcal{N}_d} \phi_{dh} \left\| \mathbf{w}_d - \hat{\mathbf{w}}_d^h \right\|^2 \\ &= \mathbb{E}\left[e_{\mathbf{v},d}^2(n)\right] + \lambda_d \sum_{h\in\mathcal{N}_d} \phi_{dh} \left\| \boldsymbol{\Omega}_d^d \boldsymbol{\varphi}_d - \boldsymbol{\Omega}_d^h \boldsymbol{\psi}_h \right\|^2, \end{aligned} \tag{12}$$

where the superscript $^{\mathrm{AD}}$ indicates the Augmented Diffusion strategy. $\boldsymbol{\varphi}_d = \mathrm{col}\{\mathbf{w}_h\}, h\in\mathcal{N}_d$ denotes the augmented control filter. $\boldsymbol{\psi}_d = \mathrm{col}\{\hat{\mathbf{w}}_h^d\}, h\in\mathcal{N}_d$ represents the local estimate of the augmented control filter based on the local virtual error signals. The coefficients $\lambda_d$ and $\phi_{dh}$ are used to balance the local error estimation term and the neighborhood regularization term. The selection matrix $\boldsymbol{\Omega}_h^d \in \mathbb{R}^{|\mathcal{N}_d|U\times U}$ is employed to select the node-specific control filter $\mathbf{w}_h$ from the augmented control filter $\boldsymbol{\varphi}_d$, and the same applies to $\boldsymbol{\psi}_d$.

By applying the Augmented Adapt-Then-Combine (AATC) strategy to the cost function in (12), the corresponding adaptation and combination equations are given by

$$\boldsymbol{\psi}_d(n+1) = \boldsymbol{\varphi}_d(n) - \mu_d^{\mathrm{AD}} \boldsymbol{\Gamma}_d(n) e_{\mathbf{v},d}(n) \tag{13}$$

and

$$\begin{aligned} \mathbf{w}_d(n+1) &= \hat{\mathbf{w}}_d^d(n+1) - \mu_d^{\mathrm{AD}} \lambda_d \sum_{h\in\mathcal{N}_d} \phi_{dh} \left[ \mathbf{w}_d(n) - \hat{\mathbf{w}}_d^h(n) \right] \\ &\approx \hat{\mathbf{w}}_d^d(n+1) - \mu_d^{\mathrm{AD}} \lambda_d \\ &\quad \times \sum_{h\in\mathcal{N}_d} \phi_{dh} \left[ \boldsymbol{\Omega}_d^d \boldsymbol{\psi}_d(n+1) - \boldsymbol{\Omega}_d^h \boldsymbol{\psi}_h(n+1) \right]. \end{aligned} \tag{14}$$

where $\boldsymbol{\Gamma}_d(n) = \mathrm{col}\{\mathbf{x}_{\mathbf{F},(d,\mathcal{N}_d)}\}$ denotes the augmented filtered-reference signal vector. Equation (14) indicates that the node-specific combination requires the updated neighborhood augmented control filter estimates $\boldsymbol{\psi}_{h\in\mathcal{N}_d}(n+1)$. However, referring to (13) and (10), this estimation depends on contributions from all nodes, as the estimation $\hat{e}_{\mathbf{v},d}(n)$ requires local information from each node. Therefore, adaptation equation should be further decomposed into the network-wide adaptation phase and the neighborhood-wide adaptation phase. The corresponding equations are given by

$$\Delta\boldsymbol{\psi}_{h\in\mathcal{N}_d}^a(n+1) = \mu_d^{\mathrm{AD}} \boldsymbol{\Gamma}_d(n) \hat{e}_{(\mathbf{v},h\in\mathcal{N}_d)(\mathbf{p},a)}(n) \tag{15}$$

and

$$\boldsymbol{\psi}_{h\in\mathcal{N}_d}(n+1) = \boldsymbol{\varphi}_{h\in\mathcal{N}_d}(n) - \sum_{a=1}^{A} \Delta\boldsymbol{\psi}_{h\in\mathcal{N}_d}^a(n+1). \tag{16}$$

Substituting Eqs. (15) and (16) into Eq. (14) yields the node-specific combination equation

$$\mathbf{w}_d(n+1) = \sum_{h\in\mathcal{N}_d} \boldsymbol{\Lambda}_{dh} \boldsymbol{\psi}_h(n+1), \tag{17}$$

where the combination matrix $\boldsymbol{\Lambda}_{dh} \in \mathbb{R}^{|\mathcal{N}_h|U\times U}$ is defined as $\boldsymbol{\Lambda}_{dh} = [\alpha_{dh,1} \;\; \alpha_{dh,2} \;\; \cdots \;\; \alpha_{dh,|\mathcal{N}_p|}] \otimes \mathbf{I}_U$. The operator $\otimes$ denotes the Kronecker product and $\mathbf{I}_U$ is the $U\times U$ identity matrix. The non-negative coefficients in the combination matrix $\boldsymbol{\Lambda}_{dh} \in \mathbb{R}^{|\mathcal{N}_h|U\times U}$ satisfy the following condition

$$\begin{cases} \sum_{h\in\mathcal{N}_d} \alpha_{dh,k} = 1, \mathcal{N}_h(k) = d, \\ \alpha_{dh,k} = 0, \mathcal{N}_h(k) \neq d. \end{cases} \tag{18}$$

Once node $d$ completes the node-specific combination phase, the updated control filter $\mathbf{w}_d(n+1)$ is transmitted to its neighboring nodes $h\in\mathcal{N}_d$ to reconstruct the augmented control filters required for the next iteration of the neighborhood-wide adaptation phase according to Eq. (16).

In summary, Eqs. (15), (16), and (17) together constitute the three iterative steps of the ADRMT as illustrated in Fig. 2(c), which are performed continuously until the system converges.

## IV. Simulations and Discussion

An 8-channel ANC headrest system was implemented in a meeting room. As shown in Fig. 3, the system comprises four ANC headrests, each equipped with a pair of secondary loudspeakers and physical microphones. In Fig. 3(a), distributed nodes No. 1 to No. 8 are arranged from left to right, with each node containing one secondary loudspeaker, one physical microphone, and one virtual microphone. In the IRMT scheme, nodes No. 1 to No. 8 form a serial communication network. In the ADRMT scheme, the nearest three nodes constitute a neighborhood (i.e., $|\mathcal{N}_d| = 3$). An integrated

processor based on the TMS320C6678 DSP chip was used to measure the acoustic paths between loudspeakers and microphones, with each path comprising 512 taps. A Brüel & Kjaer 3053 PULSE recorder was used to record the primary noise signals at both physical and virtual microphones for observation path estimation [9] , with a measured path length of 600 taps.

The normalized residual noise was used to evaluate the noise reduction performance of different schemes, defined as

$$\varsigma(n)=10\log_{10}\left[\left(\sum_{m=1}^{M}e_{\mathrm{v},m}^{2}(n)\right)\Big/\left(\sum_{m=1}^{M}b_{\mathrm{v},m}^{2}(n)\right)\right], \quad (19)$$

where $M=8$ and $M=1$ correspond to the global system and local node noise reduction performance, respectively. Here, $e_{\mathrm{v},m}(n)$ and $d_{\mathrm{v},m}(n)$ denote the residual noise and primary noise signals at the virtual microphone, respectively. Figures 4(a) and 4(b) illustrate the global and local noise reduction performance of various schemes. The proposed ADRMT algorithm achieves steady-state performance comparable to CRMT and IRMT at both the system-wide and per-node scales. IRMT exhibits a convergence rate similar to CRMT, as both essentially follow the same global filter adaptation formulation defined in (11). In contrast, ADRMT converges more slowly due to its reliance on neighborhood-based cooperation, which restricts access to global noise field information and delays its convergence.

Theoretical analyses of the per-processor computational complexity for different RMT schemes are summarized in Table I, while Fig. 5 presents the corresponding multiplication and addition operations under 8, 16, 32, and 64-channel configurations. For the 8-channel ANC headrest system shown in Fig. 3, the proposed ADRMT requires only 22.22% of the multiplications and 21.93% of the additions compared to CRMT, and 49.92% and 49.27% compared to IRMT, respectively. The computational advantage of ADRMT becomes more pronounced as the number of channels increases. Specifically, for the 64-channel case, ADRMT reduces the multiplication and addition operations to merely 2.74% and 2.73% of CRMT, and 7.15% and 7.14% of IRMT, respectively.

Another advantage of the proposed ADRMT lies in its use of a parallel diffusion strategy, which yields lower communication latency than the incremental strategy adopted by IRMT. Assuming each data transmission takes $\Delta_t$ seconds, The communication delay of IRMT is $2A(A-1)U\Delta_t$ (e.g., $573,442\Delta_t$ for the 8-channel system in Fig. 3), which increases quadratically with the number of channels. In contrast, the communication delay of ADRMT is $(|\mathcal{N}_d|+2)U\Delta_t$ (e.g., $2,560\Delta_t$ for the same system), depending only on the neighborhood number. Therefore, ADRMT can effectively mitigate communication latency in large-scale systems, thereby reducing the risk of noise reduction performance degradation caused by signal delays.

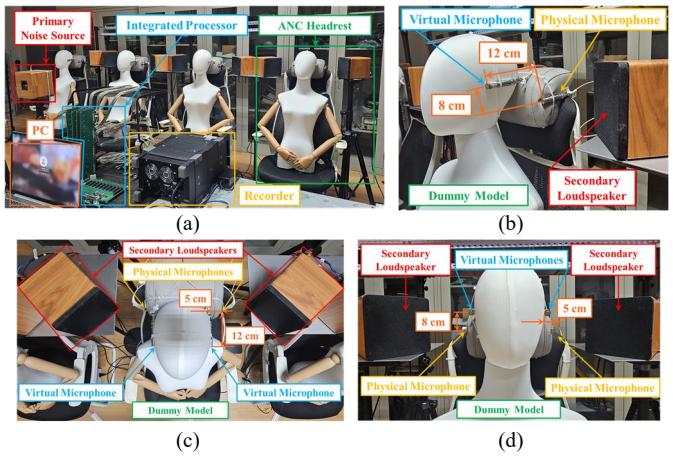


Fig. 3 Configuration of the ANC headrest system used for simulation experiments. (a) Experiment instruments; (b) Side view of the ANC headrest; (c) Top view of the ANC headrest; (d) Front view of the ANC headrest.

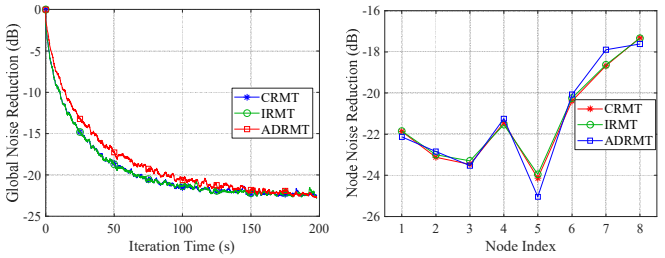


Fig. 4 Global and node-wise noise reduction performance of different RMT methods: (a) Convergence of global noise reduction; (b) Steady-state node-wise noise reduction.

TABLE I

PER-PROCESSOR COMPUTATIONAL COMPLEXITY

| | Multiplications | Additions |
|---|---|---|
| CRMT | $A^2(2R+2Q-1+U)$ $+A(U+1)$ | $A^2(2R+2Q-4+U)$ $+A(U-1)$ |
| IRMT | $A^2(Q+U)$ $+\mathrm{A}(2R+Q)+U$ | $A^2(Q+U-1)+U-1$ $+A(2R+Q-3)$ |
| ADRMT | $\sum_{d=1}^{A}[\lvert\mathcal{N}_d\rvert(Q+U)]$ $+A(2R+Q)+\lvert\mathcal{N}_d\rvert U$ | $\sum_{d=1}^{A}\lvert\mathcal{N}_d\rvert(Q-1)+\lvert\mathcal{N}_d\rvert AU$ $+(\lvert\mathcal{N}_d\rvert-1)U+A(2R+Q-3)$ |

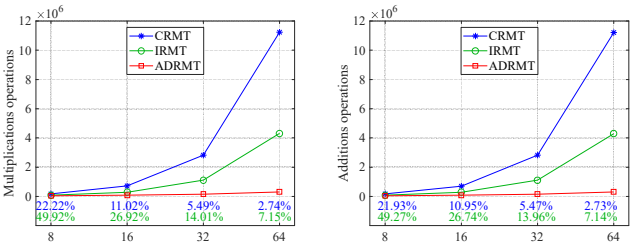


Fig. 5. Computational complexity comparison with (a) multiplication and (b) addition operations under different channel configurations

## V. CONCLUSIONS

This paper presented an augmented diffusion remote microphone technique (ADRMT) for distributed active noise control systems. By incorporating network-wide adaptation,

neighborhood-wide adaptation, and node-specific combination, ADRMT enables the precise estimation of virtual error signals and facilitates efficient noise attenuation at designated target locations. In contrast to the IRMT, which employs a serial communication and global information propagation, ADRMT utilizes a parallel communication to reduce communication latency and adopts neighborhood-based collaboration to substantially reduce computational complexity. Simulation results on an 8-channel ANC headrest system confirm that ADRMT attains steady-state noise reduction performance comparable to both CRMT and IRMT schemes, while significantly reducing computational load and communication latency. Future work will focus on real-time experimental validation of ADRMT and the development of advanced RMT schemes with improved computational and communication efficiency for large-scale distributed ANC systems.

## VI. Acknowledgment

This work was supported by the National Natural Science Foundation of China (Grants No. 12274221), the Postgraduate Research &·Practice Innovation Program of Jiangsu Province (Grants No. KYCX25_0160) and the Program of China Scholarship Council (Grants No. 202506190033).

## References

[1] S. Lian *et al.*, "An online decoupling-whitening frequency domain filtered-error least mean square algorithm for active road noise control," *J. Acoust. Soc. Am.,* vol. 156, no. 2, pp. 1413-1424, 2024.

[2] S. Lian, T. Li, S. Sun, S. Wang, and J. Lu, "A computational-efficient adaptive algorithm based on frequency point selection in multichannel active noise control systems," *Mech. Syst. Signal Process. ,* vol. 238, p. 113176, 2025.

[3] I. Dimino, C. Colangeli, J. Cuenca, P. Vitiello, and M. Barbarino, "Active noise control for aircraft cabin seats," *Applied Sciences,* vol. 12, no. 11, p. 5610, 2022.

[4] S. Zhao, X. Qiu, J. Lacey, and S. Maisch, "Configuring fixed-coefficient active control systems for traffic noise reduction," *Build. Environ.,* vol. 149, pp. 415-427, 2018.

[5] D. Moreau, B. Cazzolato, A. Zander, and C. Petersen, "A review of virtual sensing algorithms for active noise control," *Algorithms,* vol. 1, no. 2, pp. 69-99, 2008.

[6] S. Zhou, M. Wu, Z. Zhang, L. Yin, C. Wang, and J. Yang, "A low-complexity parallel local remote microphone technology for multichannel narrowband active noise control systems," *Appl. Acoust.,* vol. 227, p. 110242, 2025.

[7] S. J. Elliott and J. Cheer, "Modeling local active sound control with remote sensors in spatially random pressure fields," *J. Acoust. Soc. Am.,* vol. 137, no. 4, pp. 1936-1946, 2015.

[8] Y. Chu, M. Wu, H. Sun, J. Yang, and M. Chen, "Some Practical Acoustic Design and Typical Control Strategies for Multichannel Active Noise Control," *Appl. Sci. Basel.,* vol. 12, no. 4, 2022, Art no. 2244.

[9] C. Antoñanzas, M. Ferrer, M. de Diego, and A. Gonzalez, "Remote Microphone Technique for Active Noise Control Over Distributed Networks," *IEEE/ACM Trans. Audio, Speech, Lang. Process.,* vol. 31, pp. 1522-1535, 2023.

[10] C. Antoñanzas, M. Ferrer, A. Gonzalez, M. D. Diego, and G. Piñero, "Diffusion algorithm for active noise control in distributed networks," in *Proceedings of the 22nd Int. Conf. Sound Vibration*. 2015, pp. 776-783.

[11] J.-M. Song and P. Park, "A diffusion strategy for the multichannel active noise control system in distributed network," in *Proceedings of the Int. Conf. Comput. Sci. Comput. Intell.*, 2016, pp. 659-664.

[12] Y. Chu, S. C. Chan, C. M. Mak, and M. Wu, "A diffusion FXLMS algorithm for multi-channel active noise control and variable spatial smoothing," in *Proc. IEEE Int. Conf. Acoust., Speech, Signal Process.*, 2021, pp. 4695-4699.

[13] T. Li, S. Lian, S. Zhao, J. Lu, and I. S. Burnett, "Distributed Active Noise Control Based on an Augmented Diffusion FxLMS Algorithm," *IEEE/ACM Trans. Audio, Speech, Lang. Process.,* vol. 31, pp. 1449-1463, 2023.

[14] T. Li, S. Zhao, K. Chen, and J. Lu, "A diffusion filtered-x affine projection algorithm for distributed active noise control," in *Proc. InterNoise23*. 2023, pp. 3050-3057.

[15] T. Li *et al.*, "Experimental study of a distributed active noise control system with multi-device nodes based on augmented diffusion strategy," *J. Acoust. Soc. Am.,* vol. 156, no. 5, pp. 3246-3259, 2024.

[16] J. Ji, D. Shi, and W.-S. Gan, "Mixed-Gradients Distributed Filtered Reference Least Mean Square Algorithm–A Robust Distributed Multichannel Active Noise Control Algorithm," *IEEE Transactions on Audio, Speech and Language Processing,* 2025.

[17] J. Cheer, S. J. Elliott, E. Oh, and J. Jeong, "Application of the remote microphone method to active noise control in a mobile phone," *J. Acoust. Soc. Am.,* vol. 143, no. 4, pp. 2142-2151, 2018.

[18] S. Lian *et al.*, "Frequency domain online secondary path modelling for active noise control without auxiliary noise," in *Proc. InterNoise23*. 2023, pp. 3041-3049.

[19] R. Sun, T. Li, X. Zeng, H. Zou, K. Chen, and J. Lu, "Quasi-Newton simultaneous perturbation stochastic approximation algorithm for broadband active noise control (L)," *J. Acoust. Soc. Am.,* vol. 157, no. 6, pp. 4461-4467, 2025.

[20] L. Rao, T. Li, C. Lei, H. Zou, and J. Lu, "An online modeling and control algorithm for narrowband active noise control," *Appl. Acoust.,* vol. 241, p. 111011, 2026.

[21] S. J. Elliott, *Signal Processing for Active Control*. London, U.K.: Academic, 2001, pp. 1-270.

[22] T. Li, L. Rao, S. Zhao, H. Duan, J. Lu, and I. S. Burnett, "An augmented diffusion algorithm with bidirectional communication for a distributed active noise control system," *J. Acoust. Soc. Am.,* vol. 154, no. 6, pp. 3568-3579, 2023.

[23] T. Li, S. Zhao, Y. Huang, J. Lu, and I. S. Burnett, "A distributed adaptive wave field synthesis system," *J. Acoust. Soc. Am.,* vol. 157, no. 3, pp. 2221-2235, 2025.